SIMS Proceedings Papers

SURFACE and INTERFACE ANALYSIS

Received: 28 September 2009 Revised: 2 March 2010 Accepted: 12 March 2010 Published online in Wiley Online Library: 19 May 2010

(wileyonlinelibrary.com) DOI 10.1002/sia.3409

Fundamental studies of molecular depth profiling using organic delta layers as model systems

C. Lu,[a]* A. Wucher[b] and N. Winograd[a]

Alternating Langmuir–Blodgett multilayers of barium arachidate (AA) and barium dimyristoyl phosphatidate (DMPA) were used to elucidate the factors that control depth resolution in molecular depth profiling experiments. More specifically, thin (4.4 nm) layers of DMPA were embedded in relatively thick (~50 nm) multilayer stacks of AA, resulting in a well-defined delta-layer model system closely resembling a biological membrane. This system was subjected to a three-dimensional imaging depth profile analysis using a focused buckminsterfullerene (C_{60}) cluster ion beam. The depth response function measured in these experiments exhibits similar features as those determined in inorganic depth profiling: namely, an asymmetric shape with quasi-exponential leading and trailing edges and a central Gaussian peak. The magnitude of the corresponding characteristic rise and decay lengths is found to be 5 and 16 nm, respectively, while the total half width of the response function characterizing the apparent depth resolution was about 29 nm. Ion-induced mixing is proposed to be largely responsible for the broadening, rather than topography, as determined by atomic force microscopy.

Keywords: molecular depth profiling; SIMS; C_{60}; delta layer; Langmuir-Blodgett film

Introduction

Cluster projectiles have expanded the potential applications of secondary ion mass spectrometry (SIMS) for material characterization.[1] By combining molecular depth profiling with SIMS imaging, three-dimensional imaging is feasible, which will provide valuable information about biological samples.[2,3] Hence, it is important to investigate the factors affecting achievable depth resolution, especially for organic–organic interfaces. Since Langmuir–Blodgett (LB) films have a well-defined structure and sharp interfaces between layers, we have employed multilayer films of barium arachidate (AA) and dimyristoyl phosphatidate (DMPA) to study the fundamentals of molecular depth profiling.[4] We synthesized a 4.4-nm layer of DMPA embedded in two ~50-nm multilayer stacks of AA on a bare silicon wafer to create a delta-layer model system for characterization with a C_{60}^+ probe. As demonstrated by Shard *et al*.,[5–7] such systems are ideally suited to investigate the depth-profiling characteristics of organic films in the same way as has been done for many years in inorganic sputter depth profiling. The measured depth response function is analyzed in terms of quasi-exponential leading and trailing edges connected by a central Gaussian function as suggested by Dowsett.[8] In order to determine the influence of bombardment-induced topography formation on the measured depth resolution, the surface roughness was studied both at the original film and after sputter erosion down to the delta. Comparison of the surface topography data with the measured depth response function shows that ion-induced mixing at the organic–organic interface is the dominant factor determining the apparent depth resolution for this system.

Experimental

The preparation of the LB films has been described in detail elsewhere.[9] A single-crystal (1 0 0) silicon wafer was used as the substrate for all LB films. The substrates were treated with ozone for 10 min and rinsed with high-purity water several times to ensure hydrophilicity of the Si/SiO_2 surface. A Kibron μTrough S-LB (Helsinki, Finland) was used for multilayer LB film preparation. These films are stable in ambient conditions for over 6 months as indicated by their color, mass spectra and depth profiles. The surface roughness and crater depth after sputter depth profiling were measured by a KLA-Tencor Nanopics 2100 atomic force profilometer operated in tapping mode. Topography images were taken within 15 min, 30 min, 1 h and 1 day sequentially after the depth profile analysis and no significant difference in topography was found as a function of time after sputtering.

Sputter depth profiling was performed in a time-of-flight (ToF) SIMS instrument equipped with a fullerene cluster ion source (IOG 40–60, Ionoptika, Southampton, UK), directed at a 40° angle relative to the surface normal. Details of this instrumentation have been described elsewhere.[10] The source was operated with a focused (~7 μm diameter) 40-keV C_{60}^+ ion beam. For depth profiling, the C_{60}^+ ion beam was operated in d.c. mode to erode through the film at an area of 400 × 500 μm in 3-s intervals. Between erosion cycles, SIMS images were acquired from the same area using the pulsed C_{60}^+ projectile beam at an ion fluence of 10^{10} cm^{-2}, and ToF mass spectra were retrospectively extracted from the image data from an area of 300 × 400 μm inside the sputtered region.

* *Correspondence to: C. Lu, Department of Chemistry, Pennsylvania State University, 104 Chemistry Building, University Park, PA 16802, USA. E-mail: cxl423@psu.edu*

a *Department of Chemistry, Pennsylvania State University, University Park, PA 16802, USA*

b *Faculty of Physics, University Duisburg-Essen, 47048 Duisburg, Germany*

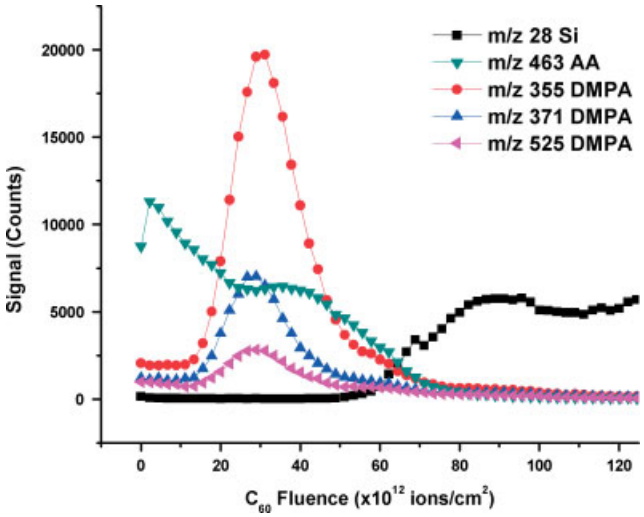

Figure 1. Secondary ion signals representing AA and DMPA *versus* fluence of the eroding C_{60}^+ ion beam.

Results and Discussion

The dependence of relevant secondary ion signals on the fluence of the eroding C_{60}^+ ion beam is shown in Fig. 1. As with our previous studies on this system,[4] the molecule-specific signals at *m/z* 463 and 525 were used to represent the AA and DMPA films, respectively. In addition, fragment ion peaks were analyzed at *m/z* 355 and 371, which are found to be specific for DMPA as well. As described earlier, the peaks detected at the DMPA-specific masses contain contributions arising from AA as well.[4] To correct for any interfering intensity, the ratio of *m/z* 355, 371 and 525, respectively, to the *m/z* 463 peak was averaged in the region where no DMPA was present. Corrected intensities of DMPA were calculated by subtracting background from AA using these ratios and the *m/z* 463 signal while profiling through the DMPA film.

In order to convert the projectile ion fluence into eroded depth, a protocol was invoked which involves a linear interpolation of the erosion rate between values determined for pure AA and DMPA films, respectively. The momentary erosion rate was calculated as

$$\frac{dz}{df} = \frac{S_{DMPA}}{S_{DMPA}^{max}} \frac{dz}{df}\bigg|_{DMPA} + \left(1 - \frac{S_{DMPA}}{S_{DMPA}^{max}}\right) \frac{dz}{df}\bigg|_{AA} \quad (1)$$

using the background-corrected DMPA signal (*m/z* 525) along with its maximum value in the delta layer. From the previously determined ratio between the erosion rates $\dot{z}_{DMPA}/\dot{z}_{AA} = 0.75$, under the bombardment conditions applied here yields

$$\frac{dz}{df} = \left(1 - 0.25\frac{S_{DMPA}}{S_{DMPA}^{max}}\right) \frac{dz}{df}\bigg|_{AA} \quad (2)$$

which was used to determine the pure AA erosion rate value from the known film thickness and the fluence needed to erode the entire film. The interface to the underlying Si substrate was identified by the point where the AA signal had decreased to 50% of its value throughout the removal of the DMPA-doped film.

The background-subtracted signals characterizing the DMPA delta layer are shown as a function of eroded depth in Fig. 2. For better comparison, the signals have been normalized to their respective maxima in Fig. 2(a). As expected from the film deposition process, the signal maxima are found at a depth of about 56 nm. The half width of the signal response function was determined as ~29 nm. This value is much larger than the real width of the delta layer (4.4 nm) and therefore characterizes the depth resolution of the experiment.

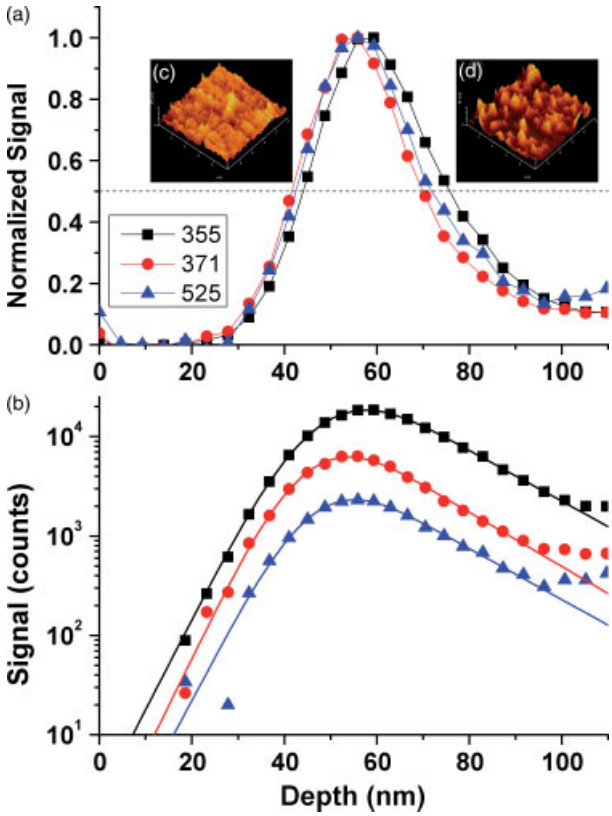

Figure 2. Secondary ion signals representing the DMPA delta layer (after subtraction of AA induced background) *versus* eroded depth. (a) Normalized to the respective signal maxima; (b) as measured. The solid lines in panel (b) represent the least square fits of the Dowsett[7] delta response function to the data (see text); (c) AFM images taken at the original film surface; (d) AFM image of the crater bottom taken at the depth of the signal maxima visible in (a).

It is interesting to note that neither the maxima nor the half width of the three signals representing the DMPA layer exactly coincides. As shown in Table 1, there is a trend that the signal peaks at larger depth and exhibits a smaller half width with decreasing size of the characteristic molecular fragment. We speculate that the reason for this behavior is that the fragment signals might be lagging behind the molecular ion signal, since a threshold ion fluence may be required to build up the damage that produce the detected fragment ions once the delta layer is reached.

In order to analyze the depth response function in more detail, a logarithmic plot of the DMPA signals is shown in Fig. 2(b). It is seen that the signal response contains exponential leading and trailing edges connected by a rounded top. Response functions of this kind are generally observed during sputter depth profiling of delta dopant structures in semiconductors.[8] They can be described by Dowsett's semiempirical function:[8]

$$R(z') = N\left[(1 - \mathrm{erf}(\xi_1))\exp\left(\frac{z'}{\lambda_g} + \frac{2\sigma^2}{4\lambda_g{}^2}\right) + (1 + erf(\xi_2))\exp\left(\frac{z'}{\lambda_d} - \frac{2\sigma^2}{4\lambda_d{}^2}\right)\right] \quad (3)$$

SURFACE and INTERFACE ANALYSIS

Table 1. Characteristic parameters characterizing the depth response function for a 4.4-nm DMPA delta layer embedded in an AA matrix

m/z	Max	FWHM	λ_g	λ_d	σ	z_0
355	57.5	28.4	4.8	17.0	8.3	53.9
371	55.9	29.4	4.8	15.0	7.5	51.3
525	54.1	31.4	5.0	16.9	7.4	51.8
Ave	55.8 ± 1.7	29.7 ± 1.5	4.9 ± 0.1	16.3 ± 1.1	7.7 ± 0.5	52.3 ± 1.4

All values are given in nanometers. FWHM, full width at half maximum.

with $\xi_1 = \frac{1}{\sqrt{2}}\left(\frac{z'}{\sigma} + \frac{\sigma}{\lambda_g}\right)$ and $\xi_2 = \frac{1}{\sqrt{2}}\left(\frac{z'}{\sigma} - \frac{\sigma}{\lambda_d}\right)$, where λ_g and λ_d are the leading and trailing edge growth and decay lengths, while σ denotes the standard deviation of a central Gaussian connecting the two exponential functions. The depth z' is referenced to the original position z_0 of the delta layer, which in our case should be located at a depth of 56 nm below the surface.

In order to extract the parameters λ_g, λ_d and σ for the DMPA delta layer studied here, Eqn (3) was fitted to the measured signal response. The resulting curves are shown in Fig. 2(b), and the corresponding parameters are listed in Table 1. All three measured DMPA signals yield similar parameters, with the leading edge consistently being steeper than the trailing edge. The leading edge slope is generally believed to reflect the escape depth of the detected sputtered particles.[8,11] Our data therefore suggest an effective escape depth of ~5 nm, which reflects both the information depth of a static SIMS spectrum and the statistical nature of the sputtering process during ion beam erosion.[12] The trailing edge is determined by the differential escape rate of dilute analyte molecules (DMPA) in the matrix (AA).[13] One can use the erosion dynamics model[14,15] to predict

$$\lambda_d = d \times \frac{Y^{\text{tot}}}{Y_0^a + nd\sigma_{\text{D}}} \tag{4}$$

where n, d and σ_{D} denote the molecule density, altered layer thickness and damage cross section, respectively, Y^{tot} is the total sputter yield (i.e. that of the pure AA matrix) and $Y_0^a \cdot c_s^a$ describes the partial sputter yield of DMPA analyte molecules. In the absence of preferential sputtering (i.e. $Y_0^a = Y^{\text{tot}}$), the trailing edge should therefore reflect the altered layer thickness corrected by the cleanup efficiency $\varepsilon = Y^{\text{tot}}/nd\sigma_D$ as

$$\lambda_d = d \times \frac{\varepsilon}{1+\varepsilon} \tag{5}$$

With typical values of $\varepsilon \sim 1$ being reached under C_{60} bombardment, a trailing edge decay length of 16 nm would therefore correspond to an altered layer thickness of the same order, which has indeed been observed.[14]

The central Gaussian reflects a convolution of the original layer thickness and other effects influencing the depth resolution such as bombardment-induced surface topography.[8]. Note that 2.2 nm of the average σ reported in Table 1 arise from the intrinsic width of the delta layer, leaving at most 5 nm for surface roughening effects. A topography image taken at the depth corresponding to the DMPA signal maximum is shown in Fig. 2(d). The root mean square (rms) roughness obtained from this image is indeed about 5 nm. However, this value is only slightly larger than that measured at the original surface (3.5 nm, as in Fig. 2(c)), indicating that the bombardment-induced roughening effect is actually much smaller. In any case, it is evident that surface microtopography is not the dominating factor determining the depth resolution observed for the system studied here.

Conclusion

Using LB multilayer stacks, an organic delta-layer model system has been designed and depth-profiled by a 40-keV C_{60}^+ ion beam. The depth resolution obtained for this system is somewhat larger (28 nm vs 18 nm) than that reported for the Irganox delta-layer system which has been examined recently[6] and used as a reference material in a VAMAS (Versailles Project on Advanced Materials and Standards) interlaboratory study.[16] These differences suggest that the molecular properties of the organic material are important in controlling the sputtering dynamics and the resulting ion beam mixing. The LB model is particularly interesting since it closely resembles the structure of a biological membrane layer and hence provides some indication of how successful three-dimensional imaging experiments will be for these types of systems.

Acknowledgements

Financial support from the National Institute of Health under grant no. 2R01 EB002016-16, the National Science Foundation under grant no. CHE-0908226 and the Department of Energy grant no. DE-FG02-06ER15803 is acknowledged.

References

[1] N. Winograd, *Analytical Chemistry* **2005**, *77*, 142a.
[2] J. S. Fletcher, N. P. Lockyer, S. Vaidyanathan, J. C. Vickerman, *Anal. Chem.* **2007**, *79*, 2199.
[3] H. Nygren, B. Hagenhoff, P. Malmberg, M. Nilsson, K. Richter, *Microsc. Res. Tech.* **2007**, *70*, 969.
[4] L. L. Zheng, A. Wucher, N. Winograd, *J. Am. Soc. Mass Spectrom.* **2008**, *19*, 96.
[5] A. G. Shard, P. J. Brewer, F. M. Green, I. S. Gilmore, *Surf. Interface Anal.* **2007**, *39*, 294.
[6] A. G. Shard, F. M. Green, P. J. Brewer, M. P. Seah, I. S. Gilmore, *J. Phys. Chem. B* **2008**, *112*, 2596.
[7] P. Sjovall, D. Rading, S. Ray, L. Yang, A. G. Shard, *J. Phys. Chem. B* **2010**, *114*, 769.
[8] M. G. Dowsett, G. Rowlands, P. N. Allen, R. D. Barlow, *Surf. Interface Anal.* **1994**, *21*, 310.
[9] L. L. Zheng, A. Wucher, N. Winograd, *Anal. Chem.* **2008**, *80*, 7363.
[10] J. Cheng, N. Winograd, *Anal. Chem.* **2005**, *77*, 3651.
[11] H. H. Andersen, *Appl. Phys.* **1979**, *18*, 131.
[12] K. D. Krantzman, A. Wucher, *J. Phys. Chem. C*, **2010**, *114*, 5480.
[13] K. Wittmaack, *Vacuum* **1984**, *34*, 119.
[14] J. Cheng, A. Wucher, N. Winograd, *J. Phys. Chem. B* **2006**, *110*, 8329.
[15] A. Wucher, *Surf. Interface Anal.* **2008**, *40*, 1545.
[16] A. G. Shard, R. Foster, I. S. Gilmore, J. L. S. Lee, S. Ray, L. Yang, *Surf. Interface Anal.* **2010**, (submitted).

